HIGH-LATITUDE PROTON PRECIPITATION AND LIGHT-ION DENSITY PROFILES DURING THE MAGNETIC STORM INITIAL PHASE

J. L. BURCH

HIGH-LATITUDE PROTON PRECIPITATION
AND LIGHT-ION DENSITY PROFILES DURING THE
MAGNETIC STORM INITIAL PHASE

By

J. L. Burch
Laboratory for Space Physics
NASA-Goddard Space Flight Center
Greenbelt, Md.   20771

January 1973

ABSTRACT

Measurements of precipitating protons and light ion densities by experiments on OGO-4 indicate that widespread proton precipitation occurs in pre-dawn hours during the magnetic storm initial phase from the latitude of the high-latitude ion trough, or plasmapause, up to $\Lambda > 75^{\circ}$. A softening of the proton spectrum is apparent as the plasmapause is approached. The separation of the low-latitude precipitation boundaries for 7.3 kev and 23.8 kev protons is $\lesssim 1^{\circ}$, compared with a 3.6° separation which has been computed using the formulas of Gendrin and Eather and Carovillano. Consideration of probable proton drift morphology leads to the conclusion that protons are injected in pre-dawn hours, with widespread precipitation occurring in the region outside the plasmapause. Protons less energetic than ~ 7 kev drift eastward, while the more energetic protons drift westward, producing the observed dawn-dusk asymmetry for the lower-energy protons.

INTRODUCTION

It has been shown by Russell and Thorne (1970) and Cole (1970) that, near midnight, ring current protons build up just outside the plasmapause. This result was based on proton measurements near the equatorial plane on OGO-3 by Frank (1967). Russell and Thorne (1970) found further that, during the ring current decay, the equatorial proton flux maximum coincided with the expanding plasmapause. Recently, Cornwall et al (1971) have noted, from measurements on a low-altitude polar satellite, that the precipitation maximum for > 40 kev and > 80 kev protons occurred just equatorward of the field line intersecting the equatorial plasmapause. Generally, the measurements at high latitudes and in the equatorial plane which they compared were separated by several hours in local time and universal time. Nevertheless, the late evening observations did appear consistently to show a precipitation maximum inside the plasmapause. In predawn hours the precipitation maximum appeared to occur outside the plasmapause in the one case in which the precipitation maximum was located. This behavior was regarded by Cornwall et al as possibly an anomalous effect due to the wide separation in longitude of the high-latitude and equatorial measurements.

In a recent abstract, Winningham (1972) has reported precipitation of isotropic protons of ring current energies in the morning and evening hours. At lower latitudes, on field lines intersecting the equatorial plasmapause and low-altitude electron density depression, Winningham observed lower energy protons, peaked at $\alpha = 90^{\circ}$, with energies from 5 ev to 15 kev.

The purpose of the present study is to associate proton precipitation profiles measured by OGO-4 in pre-dawn hours during the initial phase of two magnetic storms with the position of the high-latitude light ion trough, or plasmapause. Comparisons with near-simultaneous measurements in the late evening sector and in the low-altitude polar cusp are made and possible proton injection and drift morphology deduced.

PROTON OBSERVATIONS ON MAY 7, 1968

Interplanetary and surface magnetic conditions for May 7, 1968 are shown in Figure 1. The initial phase of the storm began with a sudden commencement at approximately 00:30 UT. OGO-4 data from three successive high-latitude passes (4179, 4180 and 4181) were obtained during the initial phase, with pass 4179 beginning approximately 5 minutes after the sc. No significant substorm activity occurred during the entire ∼ 4 hr. period of these observations, although the interplanetary magnetic field (IMF) was southward for approximately 1½ hrs. following the sc. The IMF then turned northward and remained northward until after OGO-4 pass 4181, when it again turned southward, producing widespread substorm activity and the main phase. Only very weak proton precipitation was observed during pass 4179 (orbit shown in Figure 2) except in the region of the dayside polar cusp. However, intense proton precipitation was observed over a wide latitudinal range in pre-dawn hours during the next two passes, the first of which began approximately two hours after the sc.

Figure 3 shows the precipitation profile for pass 4180, which occurred approximately 2 hours after the sudden commencement, following the first

period of southward IMF. The satellite passed through the region of

polar cusp proton precipitation at approximately 02:23 UT. The proton

energy spectra and proton fluxes observed during this pass through the

polar cusp are typical for all passes through this region during quiet

or disturbed times. However, the complete region of polar cusp proton

precipitation could be much wider in latitude than is apparent in Figure

3, since the fluxes at lower and higher latitudes could be below the

OGO-4 thresholds, which are shown by the horizontal base lines.

In pre-dawn hours widespread proton precipitation was seen in pass

4180 near 4 hrs. MLT. This precipitation extended from at least $\Lambda = 75^\circ$

down to $\Lambda \sim 66^\circ$. Simultaneous measurements on OGO-4 of the light ion

density profile (courtesy of H. A. Taylor, Jr.) show that the He^+ density

began to rise above its low level in the high-latitude trough at precisely

the latitude of the 0.7 kev proton precipitation boundary. For these

local times it has previously been shown by Grebowsky et al (1970) that

the low-altitude light ion trough and the equatorial plasmapause lie on

the same field line.

Other features to note in Figure 3 are the hardening of the proton

energy spectrum toward lower latitudes, with a very energetic spectrum

containing significant fluxes at 23.8 kev observed near the low-latitude

cutoff. Note that the 7.3 kev fluxes have been shifted upward by a

factor of 3 in the figure, since fluxes at 7.3 and 23.8 kev were of com-

parable intensities. It is also apparent in Figure 3 that the lower

energy protons extended to lower latitudes, with the knees in the 0.7

and 23.8 kev profiles separated by $\Delta\Lambda \sim 2^\circ$.

Fluxes of 2.3 kev protons are not shown for the pre-dawn portion of pass 4180 since they were very close to the threshold level of 2×10^5 cm^{-2} $ster^{-1}$ kev^{-1} sec^{-1}, and never rose above 10^6.

The sharp contrast between the proton energy spectra seen in pass 4180 in the polar cusp and in pre-dawn hours, and the fact that the polar cusp fluxes are always seen while the pre-dawn precipitation has only been found during large magnetic storms indicate that the pre-dawn precipitation is not produced by injection through the polar cusp and subsequent westward drift.

A similar behavior of the precipitating proton and light ion density profiles was observed in pass 4181, which is shown in Figure 4. However, the separations between the precipitation boundaries are somewhat smaller than in the previous example. This pass occurred ~ 30 minutes before the start of the main phase and just before the southward turning of the interplanetary magnetic field.

INTERPRETATION

The proton precipitation behavior shown in Figures 3 and 4 is consistent, in a qualitative sense, with a model in which plasma sheet protons are convected inward toward regions of higher magnetic field strength, being energized by adiabatic compression. The observations reported here for protons with pitch angles near 0° indicate that strong pitch angle diffusion occurs from near the plasmapause out to at least $\Lambda = 75^o$ in the morning hours.

The near coincidence of the precipitation bound-
aries and the plasmapause noted in Figures 3 and 4 suggests that protons
in the equatorial plane are present only outside the plasmapause. This
is reasonable near the local time of injection, since a particle cannot
cross the plasmapause by electric field drifts. The lower energy protons
are dominated by $\bar{E} \times \bar{B}$ drifts and thus cannot cross the plasmapause. The
magnetic drifts of higher energy protons could carry them across the
plasmapause, since these drifts oppose the electric field drift due to
corotation.

Deeper penetration into the plasmasphere can occur for these more
energetic protons at local times remote from the injection region if the
plasmapause cuts across magnetic drift shells. However, the plasmapause
is aligned nearly along a constant L surface in the morning hours. There-
fore, significant crossing of the plasmapause should occur chiefly in
pre-midnight hours, as the plasmasphere bulge is approached.

The near coincidence of the plasmapause and the 0.7 kev precipitation
boundary in Figures 3 and 4 indicates that, as discussed above, the pre-
cipitation boundary probably coincides with a proton boundary in the
equatorial plane. The higher latitude precipitation boundaries at 7.3
kev and 23.8 kev could then result from the separation of equatorial
proton boundaries, or Alfvén layers, produced by coupled convection and
precipitation as described by Kennel (1969) and Wolf (1970). Alternatively,

the equatorial boundary separations could be less than the separations
between the precipitation boundaries which may then be produced as pre-
dicted by Eather and Carovillano (1971).

Eather and Carovillano noted that isotropic proton precipitation
requires that the time (τ_D) for diffusion from the edge of the equatorial
loss cone to $\alpha = 0^\circ$ must be less than one-half bounce period $(T_{\frac{1}{2}})$. In
a region of uniform background plasma density and spectral wave intensity
in a dipole field, this generally results in earthward precipitation
boundaries which lie at higher latitudes as the proton energy is increased.
Using the equations derived by Gendrin (1968) it is possible to assess
such a model in terms of the observations of Figures 3 and 4.

As mentioned above, there is evidence that the 0.7 kev precipitation
boundary coincides with an equatorial boundary and the condition $\tau_D < T_{\frac{1}{2}}$
obtains throughout the 0.7 kev population. Then, assuming that the 7.3
kev boundary results from violation of the above condition, one can pre-
dict where the condition will be violated for 23.8 kev protons, producing
a precipitation boundary at that energy.

The following assumptions are made:

(1) All pitch angle diffusion takes place in the equatorial plane
    (see Kennel and Petschek, 1966).

(2) Energy diffusion is negligible within the equatorial loss cone
    (2 - 3° wide)(see Eather and Carovillano, 1971).

(3) $v = v_\parallel$ inside the equatorial loss cone, where v and $v_\parallel$ are the
    proton velocity and velocity along $\bar{B}$, respectively.

(4) The relative magnetospheric spectral intensity $(\frac{b^2}{\Delta f})$ spectrum measured by Holzer et al (1966) is appropriate for ion cyclotron waves. Based on the mathematical fit to the data by Eather and Carovillano (1971), this relationship is,

$$\frac{b^2}{\Delta f} \propto f^{-2.56}, \quad 0.35 \text{ Hz} < f < 10 \text{ Hz}.$$

(5) The magnetic field is a perfect dipole.

(6) The 7.3 kev precipitation boundary is located at $\Lambda = 65^o$.

(7) The equatorial ion density is 1 cm^{-3}.

Requiring $\tau_D = T_{\frac{1}{2}}$ for 7.3 kev protons at $\Lambda = 65^o$ (L = 5.6), we can solve for the required ion cyclotron spectral intensity. With velocity in units of the Alfven velocity, the condition for ion cyclotron resonance is (Gendrin, 1968),

$$v_{\parallel} = \frac{v_\phi^3}{v_\phi^2 - 1} , \qquad (1)$$

where v_ϕ is the phase velocity of the wave, which is negative (anti-parallel to $v_{\parallel}$) for interactions of protons with left-hand waves. Using the diffusion coefficient derived by Gendrin (1968), the pitch angle diffusion rate can be calculated from,

$$< (\Delta\alpha)^2 > = 1.6 \times 10^{-3} (\frac{b^2}{\Delta f}) v_\phi [\frac{1}{v_{\parallel}} (1 - \frac{v_\phi v_{\parallel}}{v^2})^{\frac{1}{2}}] \Delta t . \qquad (2)$$

The equatorial loss cone for L = 5.6 is approximately 3.45^o (Eather and Carovillano, 1971). Under assumptions (2) and (3) above, we can set $\Delta\alpha = 3.45^o$ and $\Delta t = \tau_D = T_{\frac{1}{2}}$ where (Hamlin, 1961),

$$T_{\frac{1}{2}} = 29.1 \text{ L} (1.30 - 0.56 \sin \alpha_e) E^{-\frac{1}{2}} \qquad (3)$$

The resonant wave frequency in units of the proton gyrofrequency is given by $f = -(1 - v_\parallel/v_\phi)^{-1}$ (Gendrin, 1968; Kennel and Petschek, 1966). The condition $\tau_D = T_{\frac{1}{2}}$ then requires a spectral wave intensity of $0.015\gamma^2/Hz$ at the 7.3 kev resonant frequency of 1.8 Hz. This intensity is in reasonable agreement with the measurements of Holzer et al (1966) which indicated an intensity of $\sim 0.016\gamma^2/Hz$ at 1 Hz (Eather and Carovillano, 1971). Under assumption (4) above, the spectral intensity at the 23.8 kev resonant frequency (at L = 5.6) of 1.5 Hz is $.024\gamma^2/Hz$. Inserting this value into equation (2) above results in a value for τ_D of 1140 sec, while $T_{\frac{1}{2}} = 43.4$ sec. As one moves to larger values of L, $T_{\frac{1}{2}}$ increases while τ_D decreases due to the combined effects of a shrinkage of the equatorial loss cone and a decrease of the proton gyrofrequency, hence an increase in $\frac{b^2}{\Delta f}$. Equality of τ_D and $T_{\frac{1}{2}}$ for 23.8 kev protons occurs at $L \sim 7.5$ or $\Lambda \approx 68.6^o$. Therefore, under the above assumptions one would expect a 3.6^o separation between the 7.3 kev and 23.8 kev precipitation boundaries, rather than the $\lesssim 1^o$ separation seen in Figures 3 and 4. The smaller separation could result, however, if the spectral wave intensity spectrum were somewhat steeper than that measured by Holzer et al (1966).

Note in Figures 3 and 4 that a slight contraction of the plasmasphere amounting to about 1° occurred between orbits 4180 and 4181. This inward motion continued through the next OGO-4 pass, although no proton data are available. It is, therefore, unlikely that the sharp precipitation boundaries were produced by the plasmasphere expanding outward into the existing proton population, depleting it by rapid precipitation induced

by the high background plasma density of the plasmasphere. Instead, the
location of the plasmapause and the various precipitation boundaries
appear to move in concert as a result of the impressed magnetospheric
electric field, with strong pitch angle diffusion occurring throughout
the proton population.

Taking a representative plasmapause position of 65° at MLT = 3 hrs.
for Figures 3 and 4, approximate drift velocities can be calculated using
the formulas of Chen (1970) for a dipole field with corotation and dawn-
dusk electric fields. The dawn-dusk electric field appropriate to this
plasmapause location is 0.1 mv/m. Using eq. (4) of Chen (1970) for
equatorial particles, drift velocities near the plasmapause location are
westward for 7.3 and 23.8 kev protons and eastward for 0.7 and 2.3 kev
protons. Therefore, the injection region for the higher energy protons
is probably located between 3-4 hrs. MLT and dawn, since, in this simple
model the radial component of the combined electric field drifts reverses
from negative to positive at dawn, precluding any further increase of
particle energy, hence gradient drift velocity. The expected separation
of low and high energy protons in the pre-dawn quadrant should result in
a large dawn-dusk asymmetry for low energy protons. Support for this con-
clusion has been found in observations during the initial phase of another
magnetic storm on November 16, 1968.

PROTON OBSERVATIONS ON NOVEMBER 16, 1968

Interplanetary and surface magnetic conditions for November 16, 1968,
are shown in Figure 5. The initial phase of the storm began with a sudden

commencement at 0916 U.T. A series of six OGO-4 passes occurred during
the initial phase. Data from the third of these are shown in Figure 6.
Unfortunately, experiment turn-off occurred in all of these decreasing
latitude passes at too high a latitude for determination of the equator-
ward precipitation boundaries in pre-dawn hours. However, the general
pattern of widespread proton precipitation from $\Lambda < 70^o$ out to $\Lambda > 75^o$
was observed on all of these passes. Proton measurements at $\alpha \approx 30^o$ and
90° indicated the same general behavior on all six passes as is seen in
Figure 6; that is, a pitch angle distribution for 2.3 kev protons which
became more isotropic toward higher latitudes.

Late in the initial phase the successive OGO-4 orbits 7047 and 7048
provided a measurement of the dawn-dusk asymmetry in proton precipitation.
Data from Orbit 7048 are shown in Figure 7. Qualitatively similar be-
havior was observed on Orbit 7047 except that higher intensities occurred
in the later orbit as the ring current apparently began to build up.
Although intense precipitation of 7.3 and 23.8 kev protons was observed
near $\Lambda \sim 65^o$ in the evening hours, only very weak low-energy precipitation
occurred at higher latitudes where, near dawn, high fluxes of 2.3 kev
protons were seen. This large dawn-dusk asymmetry for low-energy protons
supports the predictions of the simple field model that the lower-energy
protons are dominated by eastward electric field drift. This asymmetry
also suggests that the initial phase precipitation in the morning hours
consists of freshly injected protons rather than protons which have
drifted around the earth.

There is some indication in the data shown in Figure 7 that the 23.8 kev precipitation boundary lies at lower latitudes than the 7.3 kev boundary in the evening hours, producing a hardening of the spectrum at the inner boundary. The fluxes at 0.7 kev and 2.3 kev in the evening sector were, however, too weak for determination of a precipitation boundary for these lower energy protons. A similar hardening of the proton energy spectrum at the lower boundary of precipitation has been observed near midnight by Mizera et al (1972).

CONCLUSIONS

From the proton precipitation patterns observed during two magnetic storms we infer the following qualitative behavior of proton injection during the initial phase:

(1) Injection of protons occurs in pre-dawn hours during the initial phase of magnetic storms.

(2) Widespread proton precipitation occurs in pre-dawn hours up to the plasmapause. This precipitation begins at a time between 20 minutes and 2 hours following the sudden commencement.

(3) There is a softening of the precipitated proton spectrum near the low-latitude precipitation boundary in the morning hours.

(4) Near the plasmapause, protons less energetic than about 7 kev drift eastward, while the more energetic protons drift westward.

(5) This drift motion results in widespread low-energy proton precipitation up to $\Lambda \geq 75^{\circ}$ in pre-dawn hours, with only very weak fluxes above $\Lambda \sim 65^{\circ}$ in late evening hours.

REFERENCES

Chen, A. J., Penetration of low-energy protons deep into the magneto-sphere, J. Geophys. Res., 75, 2458, 1970.

Cole, K. D., Relationship of geomagnetic fluctuations to other magneto-spheric phenomena, J. Geophys. Res., 75, 4216, 1970.

Cornwall, J. M., H. H. Hilton, and P. F. Mizera, Observations of precip-itating protons in the energy range 2.5 kev $\leq$ E $\leq$ 200 kev, J. Geophys. Res., 76, 5220, 1971.

Eather, R. H., and R. L. Carovillano, The ring current as the source region for proton auroras, Cosmic Electrodyn., 2, 105, 1971.

Frank, L. A., On the extraterrestrial ring current during geomagnetic storms, J. Geophys. Res., 72, 3753, 1967.

Gendrin, R., Pitch angle diffusion of low energy protons due to gyro-resonant interaction with hydromagnetic waves, J. Atmos. Terr. Phys., 30, 1313, 1968.

Grebowsky, J. M., N. K. Rahman, and H. A. Taylor, Jr., Comparison of coincident OGO-3 and OGO-4 hydrogen ion composition measurements, Planet. Space Sci., 18, 965, 1970.

Holzer, R. E., M. G. McLeod, and E. J. Smith, Preliminary results from the Ogo 1 search coil magnetometer: boundary positions and magnetic noise spectra, J. Geophys. Res., 71, 1481, 1966.

Kennel, C. F., Consequences of a magnetospheric plasma, Rev. Geophys., 7, 379, 1969.

Kennel, C. F., and H. E. Petschek, Limit on stably trapped particle flux, J. Geophys. Res., 71, 1, 1966.

Mizera, P. F., J. B. Blake, and J. F. Fennell, Losses of outer-zone protons, EOS, Trans. Am. Geophys. Union, 53, 1088, 1972.

Russell, C. T., and R. M. Thorne, On the structure of the inner magnetosphere, Cosmic Electrodyn., 1, 67, 1970.

Winningham, J. D., Proton fluxes observed with ISIS-1 and 2 at mid-latitudes and their association with the plasmapause and SAR-arcs, EOS, Trans. Am. Geophys. Union, 53, 489, 1972.

Wolf, R. A., Effects of ionospheric conductivity on convective flow of plasma in the magnetosphere, J. Geophys. Res., 75, 4677, 1970.

FIGURE CAPTIONS

Figure 1. Summary of conditions in the interplanetary and surface magnetic fields on 7 May 1968. A sudden commencement occurred at 0030 UT.

Figure 2. Λ-MLT plots of OGO-4 polar passes discussed herein.

Figure 3. Differential proton fluxes and He$^+$ ion densities observed by experiments on OGO-4 during the northern polar pass of Orbit 4180 on 7 May 1968. Polar cusp proton fluxes were observed near 13 hrs. MLT. All proton fluxes were measured by detectors viewing radially outward from the earth (i.e., $\alpha \approx 0^o$). Note that the 7.3 kev fluxes have been shifted upward for clarity.

Figure 4. Differential proton fluxes and He$^+$ ion densities observed by experiments on OGO-4 during the northern polar pass of Orbit 4181. All proton fluxes were measured by detectors viewing radially outward from the earth (i.e., $\alpha \approx 0^o$). Note that the 7.3 kev fluxes have been shifted upward for clarity.

Figure 5. Summary of conditions in the interplanetary and surface magnetic fields on 16 Nov. 1968. A sudden commencement occurred at 0917 UT.

Figure 6. Differential proton fluxes observed by OGO-4 during the northern polar pass of Orbit 7046 on 16 Nov. 1968. Note that the 2.3 kev fluxes have been shifted upward for clarity.

Figure 7. Differential proton fluxes observed by OGO-4 during the northern polar pass or Orbit 7048 on 16 Nov. 1968. Note that the 2.3 kev and 7.3 kev fluxes have been shifted upward for clarity.
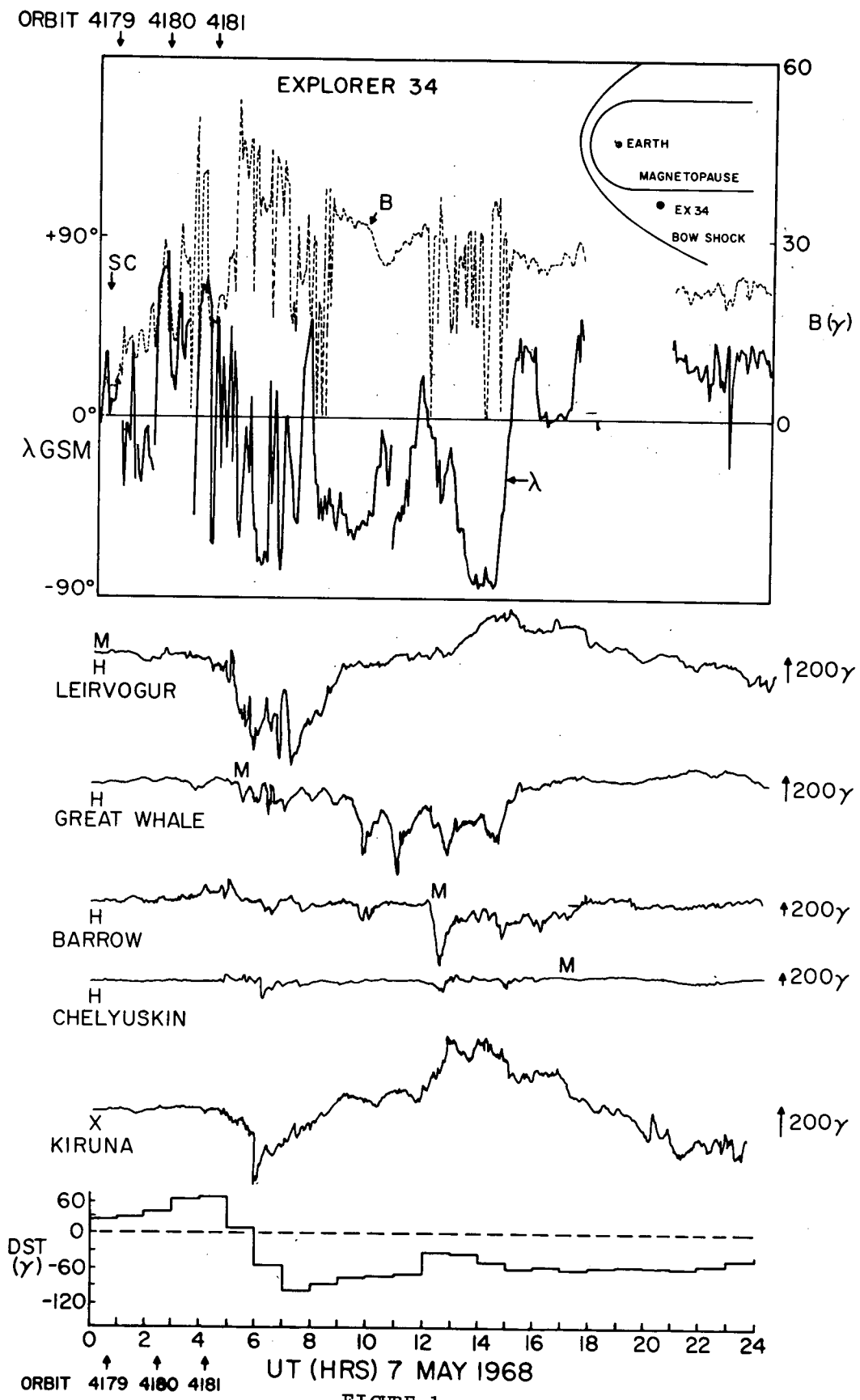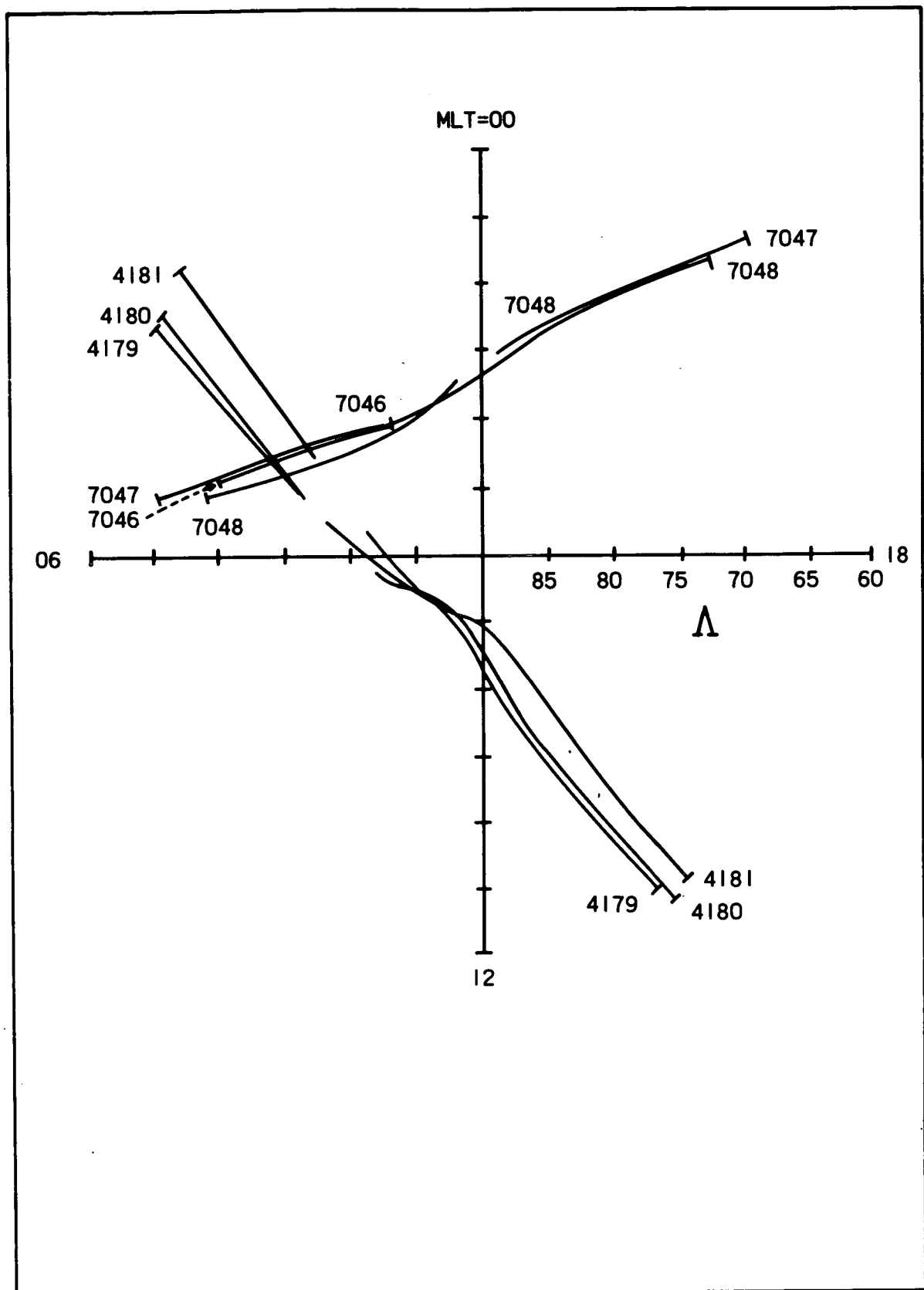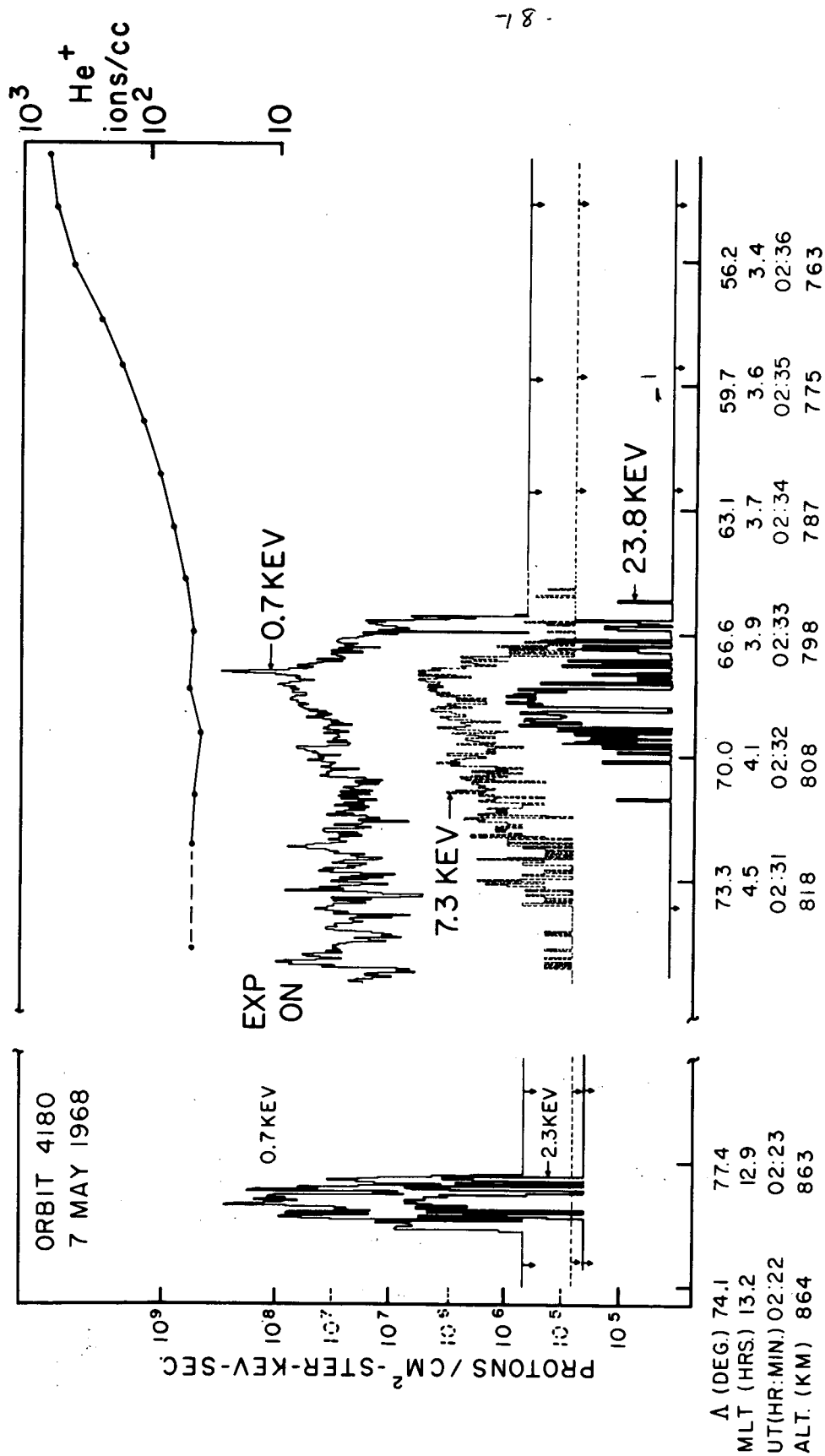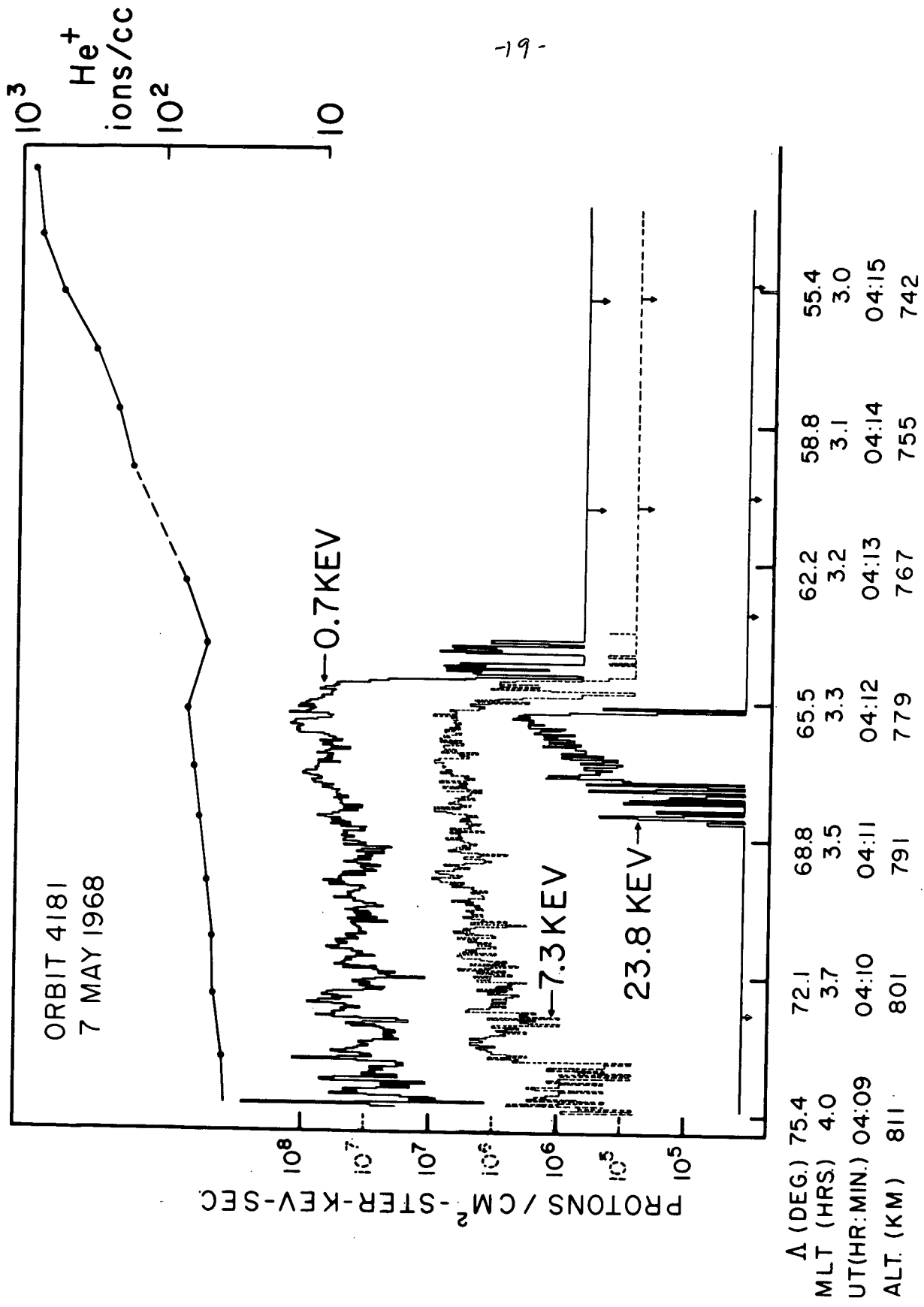
FIGURE 1

FIGURE 2

FIGURE 3

FIGURE 4

FIGURE 5

FIGURE 6

FIGURE 5

FIGURE 7

NASA-GSFC